Temperature-dependent electron mobility and large polaron interpretation in $Bi_{12}SiO_{20}$

Marc Wintermantel and Ivan Biaggio*
Nonlinear Optics Laboratory, Institute of Quantum Electronics, Swiss Federal Institute of Technology, ETH Hönggerberg, CH-8093 Zürich, Switzerland
(Received 23 December 2002; published 24 April 2003)

The electron band mobility in $Bi_{12}SiO_{20}$ is determined down to 100 K by the holographic time of flight method. Data are presented for different crystals of different origins in the temperature range between 100 and 500 K. The observed mobility rises from $\sim 1.7\ cm^2\,V^{-1}\,s^{-1}$ at 500 K to $\sim 10\ cm^2\,V^{-1}\,s^{-1}$ at 190 K, and decreases again at lower temperature. We show that the data correspond to an intrinsic band mobility between 190 and 500 K. The temperature dependence of the mobility can be reproduced in this temperature range with a large polaron model that derives all its parameters from the experimental phonon spectrum of the material. A deviation from the large polaron prediction that takes place between 250 and 190 K, depending on the sample, can be ascribed to the influence of defects or impurities.

DOI: 10.1103/PhysRevB.67.165108 PACS number(s): 72.20.Jv, 71.38.Fp, 63.20.Kr, 42.70.Nq

I. INTRODUCTION

The intrinsic mobility of an electron moving in the conduction band of a crystal is normally limited by the band structure itself and by lattice vibrations (phonons). But in crystals with some ionic character the magnitude of the mobility can be severely reduced because the charge of the electron moving in the conduction band can polarize the lattice around it. The lattice polarization has a response time characterized by the frequency of longitudinal optical phonons, and it gives rise to a Coulomb force that hinders the movement of a drifting electron. The combination of the electron with the associated lattice polarization has been called a ''polaron.''

Cubic $Bi_{12}SiO_{20}$ (BSO) is an ionic crystal that shows a relatively strong linear electro-optic effect. It is an insulator with conduction and valence band separated by an energy of ~ 3.2 eV where charge carriers can be photoexcited from impurities with energy levels inside the band gap. Its photorefractive properties have been used in spatial light modulators and optical correlators, and for dynamic holography and wave mixing applications.

The mobility of photoexcited electrons in BSO is a central parameter for its use in applications, and it reflects interesting fundamental properties of the BSO lattice. Previous measurements in the relatively small temperature interval between room temperature and 200 °C found that the mobility decreases with increasing temperature, changing from $3.4 \pm 0.5\ cm^2\,V^{-1}\,s^{-1}$ at room temperature to about half of this value at 200 °C.[1] The small magnitude of the intrinsic mobility and its temperature dependence have been explained by arguing that the electrons form large polarons[2] and by adapting previous large polaron theories, which assumed the presence of only one optical phonon mode,[3–6] to the case of the multimode phonon spectrum of BSO.[2]

In this work we extend the previous mobility measurements in BSO by exploring the temperature dependence below room temperature and by studying the influence of different crystal growth conditions. This allows one to better judge the effectiveness of the model presented in Ref. 2—which predicts that the mobility continues to increase towards lower temperatures—and provides additional data on the electron mobility and the effects that limit its magnitude in different BSO crystals. Besides the direct value of providing a better characterization of a useful material, these results are interesting for fundamental research about charge transport processes in solids, and about the theoretical models that can be used to understand them.

In order to study the electron mobility in an insulator such as BSO it is necessary to inject enough electrons in the conduction band and to observe how fast they move under the influence of an applied field or by diffusion. In a bulk sample electrons can be injected in the conduction band by photoexcitation from donor centers with energy levels in the gap between valence and conduction bands. Even nominally undoped BSO crystals have enough such centers to allow photoexcitation of a useful electron density, but the presence of defects also leads to a relatively high density of trap levels that limits the free carrier lifetime to a few nanoseconds,[7] and can lead to the determination of an average mobility value that is limited by trapping and thermal excitation from shallow traps.[12,13] To measure the free carrier mobility it is therefore necessary to observe the electrons in the first few nanoseconds after they were photoexcited. In this work we use the Holographic Time of Flight (HTOF) method in diffusion mode.[1] In this technique both photoexcitation of electrons and the detection of their movement are done using short laser pulses on a subnanosecond time scale, which allows a contactless all-optical determination of the electron mobility.

Because of its role in our measurements, and because of the importance of a careful selection of the experimental parameters for an accurate determination of the intrinsic electron mobility, we start by giving a brief outline of the HTOF method and its principles in the next section. Then we discuss the realization of the temperature dependent HTOF measurements in the case of BSO, and finally we present and discuss the experimental results for the intrinsic electron mobility and its temperature dependence in various BSO crystals.

Holographic time of flight

The holographic time of flight method for the investigation of charge transport in insulators and semiconductors is based on the controlled photoexcitation of a spatially modulated free charge carrier distribution and on the contactless optical detection of its evolution. A light-pattern created by two-beam interference provides the inhomogeneous photoexcitation mechanism, while the electro-optic (Pockels) effect present in noncentrosymmetric materials allows for a sensitive detection of charge-displacement by transforming any space-charge electric field into a refractive index modulation. A number of techniques related to these principles have been demonstrated over the years.[1,7–12,14–20] HTOF (Refs. 1 and 9) distinguishes itself because it is based on short-pulse photoexcitation, which allows one to separate the photoexcitation from the charge-transport process temporally. The basic assumptions that enable a simple analysis of an HTOF experiment and of the data it produces are the following

(1) The photoexcitation pulses are so short that no charge transport takes place during the pulse duration.
(2) Only one type of mobile carrier is excited by photoionization of impurity centers with energies in the gap between valence and conduction band. Photoexcitation takes place in the bulk of the material.
(3) The density of photoexcited carriers is so small that there are no saturation effects during photoexcitation and that the space-charge field that is built up by subsequent charge transport has a negligible influence on the transport dynamics itself.
(4) The average lifetime τ of the photoexcited carriers is a constant (i.e., the distribution of any trapping centers can be assumed to be homogenous).

The first requirement implies the selection of an appropriate laser source with short enough pulses.

The second requirement can be fulfilled by choosing an appropriate photoexcitation wavelength that maximizes the probability for the photoexcitation of one particular carrier, and also by targeted doping of the material. Note that requirement (2) does not forbid simultaneous photoexcitation of electrons and holes as long as there is a large enough difference between their respective mobilities, and only the contribution of one carrier is observed on a given time-scale.

The third requirement (3) of a small density of photoexcited carriers is met by reducing the energy in the photoexcitation pulse. This can be easily done because the detection of charge displacement by the electro-optic effect allows a much greater sensitivity than other kinds of optical detection that rely on the change of optical properties introduced by the free-carrier density itself.

The fourth requirement (4) is met in the presence of a spatially homogeneous distribution of traps in addition to the donor centers providing the photoexcited carriers. Further, if retrapping in the original donors was a significant contribution to the free carrier lifetime τ, one can help satisfying requirement (4) by reducing the contrast in the interference pattern that photoexcites the carriers, and by the enforcement of requirement (3).

It is important to note that the above assumptions can be largely fulfilled by adjusting experimental parameters that can be easily controlled (wavelength, pulse length, pulse energy, contrast in the optical interference pattern). When requirements (1)–(4) are met, the nature of the impurity centers from which the free carriers are excited, or the nature of the trapping centers that limit their lifetime, are not important for the analysis.

It is clear that a sinusoidal distribution of free charge carriers can also modulate the optical properties of the material directly through several mechanisms such as free carrier polarizability,[21] and allow the optical detection of the evolution of the free carrier distribution even in the absence of a linear electro-optic effect. Several investigations of the evolution of charge carrier distribution published in the past have relied on such mechanisms.[22] However, a relatively high carrier density is generally required to appreciably modulate the optical properties of a material, which can lead to a number of ambiguities in the interpretation of experimental results. As an example, the space-charge fields caused by the evolution of a large free carrier density are also large, and they must be taken into account when interpreting the signal dynamics, while additional effects not connected to charge transport—temperature modulation, heat diffusion, etc.—also contribute to the signal. For small free-carrier densities and in noncentrosymmetric materials like BSO the refractive index modulation caused by the space-charge field is generally much higher than any absorption or refractive index modulation induced by the free-carriers themselves, and the HTOF method is a better choice.

The basic principles of the HTOF method can be understood using a modified form of the treatments that were first introduced in Refs. 7 and 14. We assume the photoexcited carriers to be electrons. After the excitation pulses have left the crystal at time $t=0$, the space and time dependences of the electron density can be described by

$$n(z,t)=n_0(t)+\frac{1}{2}[n_1(t)\exp(ik_{sp}z)+\text{c.c.}], \tag{1}$$

where $n_1(t)$ is a complex amplitude and the initial conditions $n_0(t=0)=n_0^0$ and $n_1(t=0)=n_1^0$ are given by the average energy and the contrast of the interference pattern used to photoexcite the carriers. k_{sp} is the modulus of the wave vector (pointing in the z direction) describing the sinusoidal interference pattern. Under the assumptions mentioned above, the time evolution $n(z,t)$ is governed by a free-carrier lifetime τ, by diffusion, and by the static field E applied along the z direction,

$$\frac{\partial n(z,t)}{\partial t}=-\frac{n(z,t)}{\tau}+\left[\frac{\mu k_B T}{e}\right]\frac{\partial^2 n(z,t)}{\partial z^2}+\mu E\frac{\partial n(z,t)}{\partial z}, \tag{2}$$

where μ is the charge-carrier mobility, k_B is Boltzmann's constant, e is the unit charge, and the "+" sign in front of the last term comes from the assumption that the mobile carriers have a negative charge.

Substituting Eq. (1) into Eq. (2), one obtains

$$n_0(t) = n_0^0 \exp(-t/\tau),$$
$$n_1(t) = n_1^0 \exp(-\Gamma t), \tag{3}$$

where $\Gamma = 1/\tau + 1/\tau_D + i\omega_E$, τ_D is the diffusion time,

$$\tau_D = \frac{e}{k_{sp}^2 \mu k_B T}, \tag{4}$$

and $\omega_E = \mu E k_{sp}$ is the rate of change of the spatial phase caused by drift in the applied field.

Using Eq. (3), we can rewrite Eq. (1) in the form

$$n(z,t) = n_0^0 \exp(-t/\tau)\left[1 + \frac{n_1^0}{n_0^0}\exp(-t/\tau_D)\cos(k_{sp}z + \omega_E t)\right], \tag{5}$$

which shows that the average carrier density decays exponentially with the free carrier lifetime, the modulation in the charge-distribution decays exponentially with the diffusion time, and the phase of the charge distribution changes linearly with the drift velocity μE.

Immediately after photoexcitation, the space-charge corresponding to the free charge carriers $[-en(z,t=0)]$ is exactly compensated by the ionized centers from where they were excited, which have a charge density $+en(z,t=0)$. The evolution of the free electron density described by Eq. (5) then uncovers the space-charge field of the ionized donors. As already mentioned above, the trapping mechanism behind the free carrier lifetime τ does not need to be described in any special way provided that its effect is just to transform a mobile free carrier described by the mobility μ into an immobile carrier. If the carrier was captured by a shallow trap, we assume that there is no significant thermal re-excitation on the time scale of the experiment (a thermal re-excitation much faster than the time scale of the experiment would be taken into account by an effective trap-limited mobility). The density of trapped charge carriers at any given time after photoexcitation is then simply given by $\partial n_T(z,t)/\partial t = -n(z,t)/\tau$. It is essentially the time integral of Eq. (5).

The space-charge electric field is found from the Gauss equation and the balance of the charge densities of ionized donors, moving electrons, and trapped electrons,

$$\frac{\partial E_{sc}(z,t)}{\partial z} = \frac{e}{\epsilon\epsilon_0}[n(z,t=0) - n(z,t) - n_T(z,t)], \tag{6}$$

and it is $E_{sc}(z,t) = [E_{sc}(t)\exp(ik_{sp}z) + c.c.]/2$, with the complex amplitude

$$E_{sc}(t) = E_{sc}^{\infty}[1 - \exp(-\Gamma t)], \tag{7}$$

where

$$E_{sc}^{\infty} = n_1^0 \frac{e}{ik_{sp}\epsilon\epsilon_0}\left[1 + \frac{1/\tau}{1/\tau_D + i\omega_E}\right]^{-1}. \tag{8}$$

In a noncentrosymmetric material, this electric field causes a spatial refractive index modulation (an holographic grating) with an amplitude that is linearly proportional to the absolute value of Eq. (7). A probe pulse diffracted off this refractive index grating has an energy proportional to $|E_{sc}(t)|^2$ and allows a direct observation of charge transport. In the HTOF method, the detected signal has a very characteristic signature, described by Eq. (7), that can be easily distinguished from other effects not connected to transport: the charge-transport signal starts growing from zero, immediately after the pump pulses leave the sample, and evolves toward a stationary value as the charge carriers diffuse and drift. When a dc electric field in the z direction is applied to the sample during the experiment, and the lifetime τ is larger than both τ_D and $1/\omega_E$, the signal oscillates in time on the way to the steady-state, with a characteristic period related to the drift velocity and the period of the spatial interference pattern.[7,9–12]

In this work no electric field was applied, which removes a possible source of uncertainty and an unnecessary experimental difficulty, and $\omega_E = 0$. Then the time oscillations of the signal are absent, and when $\tau \gg \tau_D$ the exponential buildup time is given by the diffusion time $\tau_D[\Gamma \to 1/\tau_D$, see Eqs. (7) and (4)]. This allows a determination of the free carrier mobility.[1,14,15]

Clearly, this result is only valid if the requirements described above are met, and the experimental parameters are chosen accordingly. Once the optical pulse length and wavelength have been selected, the two most important parameters in the HTOF setup that directly determine if an accurate mobility measurement is possible are the crossing angle between the pump beams and the optical energy density in the pump pulses.

The crossing angle between the beams gives the transport length and the value of the diffusion time τ_D, and determines if the condition $\tau_D \ll \tau$ is met. This condition means that the ''typical'' electron avoids shallow and deep traps for so long that the electron-distribution can become almost homogenous because of diffusion (the space-charge field built up by diffusion has been assumed to be low enough to allow for this). This can be checked experimentally by observing if the exponential rise time of the signal varies as the square of the modulation period of the photoexcited carrier distribution.

The optical pulse fluence determines the linearity of the photoexcitation process and the maximum space-charge field that the photoexcited carriers can produce when they diffuse. Too strong optical pump pulses will lead to saturation effects, which will deform the single-exponential buildup and produce shorter buildup times.[15] In the low fluence limit the observed signal rise-time does not depend on the fluence, and the diffraction efficiency of the probe pulse is proportional to the square of the total photoexcitation energy.[15]

To satisfy both requirements it is necessary to perform measurements for different crossing angles between the beams and for different pulse energies.[1,15] This allows the selection of the optimal spatial modulation period in the interference pattern, and of the optimum pulse energies which still give a good signal-to-noise ratio, but which are well below the limits above which saturation effects occur.

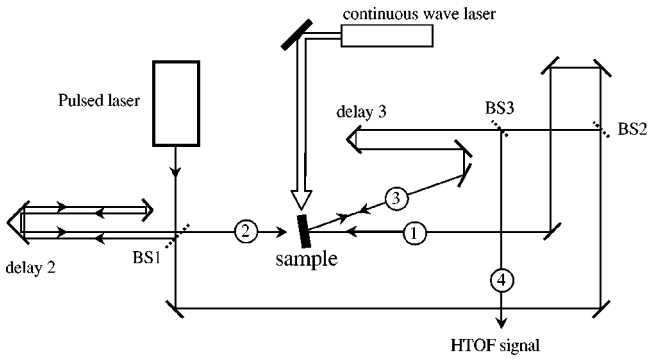

FIG. 1. (a) Degenerate four wave mixing configuration for HTOF Measurements. Beams 1 and 3 create the interference pattern which excites the inhomogeneous distribution of free carriers. Beam 2, which can be delayed, diffracts off the refractive index grating caused by charge-diffusion and leads to diffracted beam 4. A continuous wave laser illuminates the sample all the time to make sure that any space-charge modulation is completely erased by the homogenous illumination during the interval between laser pulses.

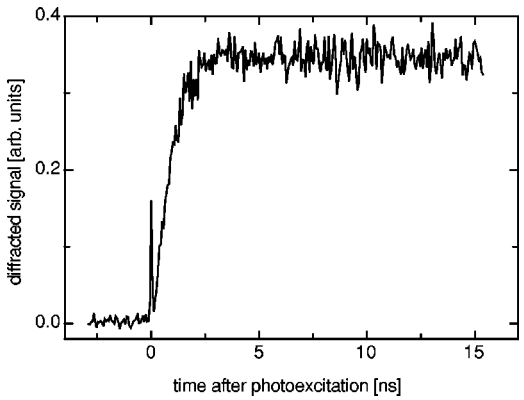

FIG. 2. Typical plot of the diffracted pulse energy vs. probe-pulse delay time obtained at room temperature for a modulation period of the interference pattern of 0.5 μm. The exponential buildup time corresponding to this measurement is 0.71 ± 0.06 ns, and it is determined by the diffusion time of the electrons. The peak observed at a delay time of zero is caused by an instantaneous third order nonlinear optical response that is not relevant for the present investigation.

II. EXPERIMENTAL

We use a frequency-doubled Nd:YAG (yttrium aluminum garnet) laser that produces 70-ps, 532-nm pulses at a repetition rate of 10 Hz. A beam splitter sends part of a pulse into a delay line, to act as a probe beam, and the other part is split again into two write pulses that arrive simultaneously in the sample, creating a spatially modulated photoexcited electron density. A scheme of the experimental setup is shown in Fig. 1.

The phase grating produced by diffusion of the photoexcited charges is detected by Bragg diffraction of the time-delayed probe pulse 2. The sample is homogeneously illuminated all the time by a 514-nm argon ion laser beam with an intensity of approximately 0.1 W/cm^2. In the time interval between two measurements, this illumination erases the space-charge induced grating created by the write pulses. During the measurement time (a few ns) this erase beam deposits six orders of magnitude less energy than the write pulses, and it does not affect the observed space-charge dynamics in the nanosecond time scale.[1]

The result of a typical measurement is shown in Fig. 2. When the probe pulse precedes the write pulses no signal is observed. When the probe pulse is delayed, the diffracted signal increases as the photoexcited electrons diffuse away from the ionized donors from which they were photoexcited, thus creating a space-charge field.

The sample was mounted inside a cold-finger helium-flow crystal from Cryo Industries with four optical windows. The temperature was stabilized by using both a needle valve to set the helium flux and a Lakeshore 330 temperature controller with two NTC (negative temperature coefficient) sensors and a heater for fine adjustment. No electrical connections besides those for the temperature control were necessary because we did not need to apply an electric field or measure a current electrically. A good heat transfer between crystal and cold finger was guaranteed by a copper holder and Apiezon heat conducting grease. The two NTC temperature sensors were mounted above and below the sample, which allowed a good control of the homogeneity of the sample temperature. A 10^{-4}-mbar insulating vacuum was maintained around the cold finger and the sample.

We performed measurements at several temperatures between 90 K and room temperature. At every temperature, we made sure that we met the requirements for a valid mobility measurement. We established that both the period and the average energy density of the photoexcitation pattern were small enough, according to the criteria discussed above. For the BSO crystals used in this study, it was found that the average fluence in the interference pattern that photoexcites the electrons must be of the order of 1 mJ/cm^2 or less, and that the diffusion-time dominates the buildup at spatial periods $2\pi/k_{sp}$ below ~ 0.5 μm. This was confirmed at all temperatures and for all samples.

The samples we investigated are shown in Table I. Two of them (called SU-1 and CT-3) are the same samples that have been used in Ref. 1 and several other works on the photorefractive properties of BSO.[23,24] The others are samples that have been grown under different conditions at the National Institute for Research in Inorganic Crystals (NIRIM), Tsukuba, Japan. One of them (AL-2) was doped with aluminum, the other one (CM) was simply grown from a congru-

TABLE I. $Bi_{12}SiO_{20}$ crystals used in this work. SU-1 and CT-3 (Refs. 1, 23, and 24) are on loan from R. W. Hellwarth, University of Southern California (USC), U.S.A. AL-3 and CM where provided by K. Kitamura, from the National Institute for Research in Inorganic Crystals (NIRIM), Tsukuba, Japan.

Sample name	Description and origin
SU-1	Sumitomo, USC
CT-3	Crystal Technology, USC
AL-3	Aluminum doped, NIRIM
CM	From a congruent melt, NIRIM

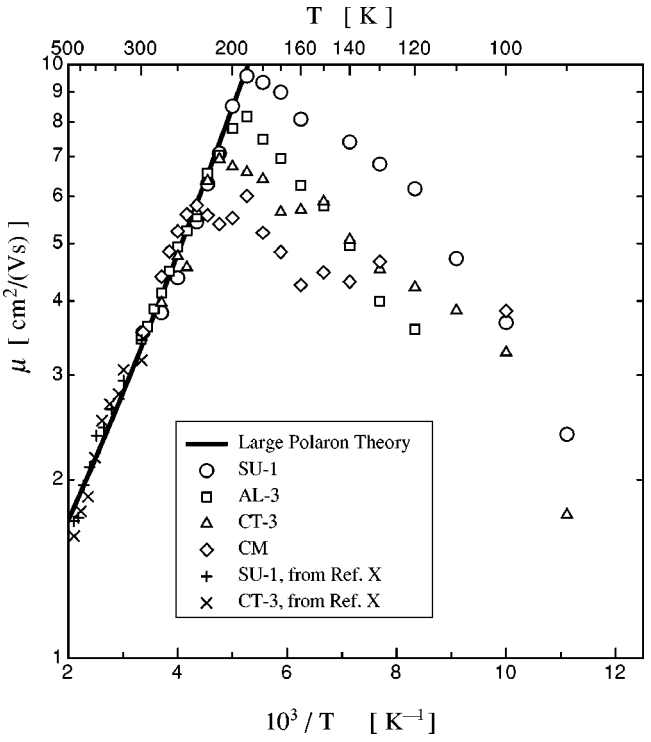

FIG. 3. Temperature dependence of the electron band mobility in various $Bi_{12}SiO_{20}$ samples. The data points at temperature higher than room temperature represented by diagonal and vertical crosses were obtained in Ref. 1. The solid line represents the prediction for large polarons, calculated using the model given in Ref. 2 from the optical phonon spectrum of BSO and using an effective electron mass of 2 electron masses. For clarity, no error bars are drawn in the figure. The error of the individual measurement was generally in the order of $\pm 10\%$.

ent melt. No precise data are available on the doping and defect structure of these samples, although all of them have been found to contain impurities leading to energy states in the gap between valence and conduction band. This variety of samples with different histories will help in differentiating effects that are intrinsic to the BSO lattice from the influence of impurities and other crystal imperfections.

III. RESULTS AND DISCUSSION

The HTOF technique described in Sec. II allowed us to observe the movements of the photoexcited carriers over a submicrosecond length scale and in the first fractions of nanoseconds after photoexcitation. Figure 3 collects all the mobility data that we determined in the crystals listed in Table I at temperatures between 100 K and room temperature. In this figure, we also include earlier measurements performed between room temperature and 500 K in Ref. 1.

All the BSO samples we studied, despite their different origins, show an identical temperature dependence between 250 and 500 K that appears to be well described by a straight line in the log-μ vs $1/T$ plot of Fig. 3. The first consequence of this observation is that in this temperature range the mobility of photoexcited electrons must be an intrinsic property of BSO, because all samples—despite their different origins—share the same temperature dependence of the mobility, and also the same absolute mobility value. A second observation is that the temperature dependence points at the interaction with phonons as the mechanism determining the electron mobility. However, the low absolute value of the mobility cannot be modeled in the relaxation time approximation, assuming independent collisions between the electron and phonons.[1,2]

A solution to this problem is provided by the fact that BSO is an ionic lattice. This suggests that the mobility is limited by the interaction of the electrons with longitudinal optical phonons. The electron polarizes the lattice around it and the Coulomb interaction with the polarized lattice tends to capture it in a self-induced potential well. This can lead to the formation of small and large polarons.[2–6] Small polarons are formed when the self-induced potential well is strong enough to capture the electron in such a way that it can free itself only by thermal excitation. In such a case the observed mobility would be characterized by an activation energy and grow exponentially with temperature. In contrast, we observed the mobility to increase toward lower temperatures between 500 and 200 K. This is consistent with an electron-phonon interaction that leads to the formation of large polarons,[2–6] where the lattice polarization induced by the electron encompasses many atoms in the crystal lattice. Reference 2 described how the large polaron model developed in Ref. 6 can be applied to the case of BSO, and how the mobility of a large polaron can be modeled from parameters derived from the experimental infrared reflectivity spectrum of BSO (Ref. 25), which gives the strength and frequencies of the optical phonon modes.

The prediction from the model described in Ref. 2 is plotted as a solid curve in Fig. 3. In this kind of semilogarithmic plot, the theoretical prediction resembles a straight line. The only free parameter in this plot is the effective mass m^* of the bare electron in the undeformed BSO lattice which was taken to be equal to 2 electron masses m_e. This effective mass essentially only determines the absolute position of the solid curve in the plot, but does not influence the predicted temperature dependence, which depends on the phonon spectrum, represented by an effective longitudinal optical phonon frequency and oscillator strength.[2] The predicted temperature dependence is in very good agreement with the experimental data on the electron mobility between 200 and 500 K.

This agreement is good for $m^*=(2\pm 0.1)m_e$, but we repeat that the value of m^* does not influence the slope of the solid curve in Fig. 3, which is almost completely given by the value of the effective longitudinal optical phonon frequency.[2] The fact that the slope of the solid curve was calculated independently makes the agreement between theory and data even more remarkable. Both this, and the fact that the experimental electron mobility and its temperature dependence are the same within the experimental error for several different BSO samples in the temperature interval between 250 and 500 K, gives support to the fact that we determined an intrinsic mobility value.

Our results therefore do two things: they confirm the validity of the theoretical approach described in Ref. 2, and they give convincing evidence that electrons in BSO form

large polarons in the temperature range above 250 K. At lower temperatures, and depending on the individual sample, the mobility deviates from the predicted large polaron behavior and starts decreasing again. This deviation occurs at the highest temperature ($\sim$235 K) for sample CM, and at the lowest temperature ($\sim$190 K) for SU-1. The systematic variations in the absolute mobility value below 250 K between the different samples is a strong indication that in this temperature range the mobility is influenced by extrinsic parameters, probably related to impurities or other defects in the crystal structure that depend on crystal growth conditions. The fact that sample CM already deviates from the intrinsic value at $\sim$235 K could be an indication of a higher defect concentration in this crystal, while the reverse would be true for SU-1. However, the exact origin of the mobilities observed below 190 K is not known at present, and any more detailed discussion is outside the scope of this work.

IV. CONCLUSIONS

In conclusion, we were able to accurately determine the temperature dependence of the intrinsic mobility of photoexcited electrons in BSO. The mobility increases with decreasing temperature, and in the best sample we observed a mobility that reached 10 $cm^2\,V^{-1}\,s^{-1}$ at 190 K before falling off again, probably because of extrinsic effects.

The experimentally observed temperature dependence above 190 K can be predicted from the experimental phonon spectrum without any free parameter by using an extension to existing large polaron theories.[2] The absolute value of the mobility can also be calculated in the same way, but does depend on the (unknown) value of the electron effective mass in BSO. We found that a good agreement with the data is reached for an effective mass equal to two electron masses. These observation are a good evidence that photoelectrons in BSO are large polarons; their observed band mobility below 250 K is intrinsic, and its small value makes photoelectrons in BSO the clearest example of such polarons found to date.

ACKNOWLEDGMENT

We thank Professor R. W. Hellwarth (University of Southern California) and Dr. K. Kitamura (Advanced Materials Laboratory, NIMS, Tsukuba) for providing us with the BSO samples. We thank Professor P. Günter (ETH Zürich) for his support during this work.

*Present address: Department of Physics, Lehigh University, Bethlehem, Pennsylvania 18015.

[1] I. Biaggio, R.W. Hellwarth, and J.P. Partanen, Phys. Rev. Lett. **78**, 891 (1997).
[2] R.W. Hellwarth and I. Biaggio, Phys. Rev. B **60**, 299 (1999).
[3] H. Fröhlich, Adv. Phys. **3**, 325 (1954).
[4] R.P. Feynman, Phys. Rev. **97**, 660 (1955).
[5] Y. Osaka, Prog. Theor. Phys. **22**, 437 (1959).
[6] R.P. Feynman, R.W. Hellwarth, C.K. Iddings, and P.M. Plazman, Phys. Rev. **127**, 1004 (1962).
[7] J.P. Partanen, P. Nouchi, J.M.C. Jonathan, and R.W. Hellwarth, Phys. Rev. B **44**, 1487 (1991).
[8] G. Pauliat, A. Villing, J.C. Launay, and G. Roosen, J. Opt. Soc. Am. B **7**, 1481 (1990).
[9] J.P. Partanen, J.M.C. Jonathan, and R.W. Hellwarth, Appl. Phys. Lett. **57**, 2404 (1990).
[10] P. Nouchi, J. P. Partanen, and R. W. Hellwarth, in Conference on Lasers and Electro-Optics, 1992, Vol. 12, OSA Technical Digest Series (Optical Society of America, Washington, DC, 1992), p. 84.
[11] P. Nouchi, J.P. Partanen, and R.W. Hellwarth, J. Opt. Soc. Am. B **9**, 1428 (1992).
[12] P. Nouchi, J.P. Partanen, and R.W. Hellwarth, Phys. Rev. B **47**, 15 581 (1992).
[13] I. Biaggio and G. Roosen, J. Opt. Soc. Am. B **13**, 2306 (1996).
[14] I. Biaggio, M. Zgonik, and P. Günter, J. Opt. Soc. Am. B **9**, 1480 (1992).
[15] M. Ewart, I. Biaggio, M. Zgonik, and P. Günter, Phys. Rev. B **49**, 5263 (1994).
[16] G.G. Malliaras, V.V. Krasnikov, H.J. Bolink, and G. Hadziioannou, Phys. Rev. B **52**, R14 324 (1995).
[17] G.G. Malliaras, V.V. Krasnikov, H.J. Bolink, and G. Hadziioannou, Appl. Phys. Lett. **67**, 455 (1995).
[18] D. Mahgerefteh, D. Kirillov, R.S. Cudney, G.D. Bacher, R.M. Pierce, and J. Feinberg, Phys. Rev. B **53**, 7094 (1996).
[19] P. Bernasconi, I. Biaggio, M. Zgonik, and P. Günter, Phys. Rev. Lett. **78**, 106 (1997).
[20] P. Bernasconi, G. Montemezzani, I. Biaggio, and P. Günter, Phys. Rev. B **56**, 12 196 (1997).
[21] R.K. Jain and M.B. Klein, in *Optical Phase Conjugation*, edited by R.A. Fisher (Academic, New York, 1983).
[22] R.I. Devlen and E.A. Schiff, J. Non-Cryst. Solids **141**, 106 (1992).
[23] Ping Xia, J.M.C. Jonathan, J.P. Partanen, and R.W. Hellwarth, Opt. Lett. **18**, 1780 (1993).
[24] F.P. Strohkendl, P. Tayebati, and R.W. Hellwarth, J. Appl. Phys. **66**, 6024 (1989).
[25] W. Wojdowski, T. Lukasiewicz, W. Nazarewicz, and J. Zmlja, Phys. Status Solidi B **94**, 649 (1979).